



Improvement in the physical properties of poly(lactic acid)/thermoplastic starch blends using oligo(lactic acid)-grafted starch

Kazuki Shibasaki¹ · Yu-I Hsu¹ · Hiroshi Uyama¹

Received: 13 March 2024 / Revised: 18 April 2024 / Accepted: 19 April 2024 / Published online: 18 June 2024
© The Author(s), under exclusive licence to The Society of Polymer Science, Japan 2024

Abstract

General-purpose petroleum-derived plastic remains in the environment for long periods and has significant impacts on oceans and land. Biodegradable and biomass plastics are being developed around the world as countermeasures. A poly(lactic acid) (PLA)/thermoplastic starch (TPS) blend is a promising ecofriendly alternative to biodegradable plastic made from plants. However, owing to the hydrophilicity of starch and the hydrophobicity of PLA, phase separation occurs between PLA and starch. Furthermore, PLA/TPS blends have poor water resistance because of the presence of starch, limiting their applications. In this study, to improve the affinity of PLA for starch, oligo(lactic acid)-grafted starch (OLAgSt) was synthesized as a compatibilizer for PLA/TPS blends, and the effect of its addition to PLA/TPS blends was evaluated. OLAgSt with different OLA molecular weights and degrees of substitution (DS) were synthesized, and their effects on PLA/TPS were compared. The results indicated that OLAgSt functioned as a good compatibilizer, improving the dispersibility of TPS in PLA with 4 wt% OLAgSt added to PLA/TPS and improving the water resistance. Moreover, the OLA molecular weight of OLAgSt was greater than that of DS. These results are expected to facilitate the development of PLA/TPS applications in the food packaging and biomedical fields.

Introduction

The environmental problems caused by the mass production and disposal of plastic products have become important issues for establishing a sustainable future. Petroleum-based plastics have significant impacts on oceans and land because they do not degrade in the environment [1, 2]. To address these issues, the development of biodegradable plastics is attracting increasing amounts of attention. Polybutylene adipate terephthalate (PBAT) and polybutylene succinate (PBS) are examples of biodegradable plastics. These materials have mechanical flexibility, similar to that of polyolefin [3]. PBAT and PBS are used industrially for agricultural films and food packaging;

however, they are derived from petroleum and do not achieve carbon neutrality. Poly(lactic acid) (PLA) is another promising alternative to biodegradable plastics and is widely known as an ecofriendly plastic synthesized from plant-derived lactic acid [4]. PLA is a biodegradable material that breaks down into CO₂ and water, making it less harmful to the environment than petroleum-based plastics [5]. Therefore, it is expected to contribute to carbon neutrality. However, PLA biodegrades only in hot and humid environments, such as compost, and may not biodegrade in environments with few microorganisms, such as the ocean [6].

In contrast, starch is easily degraded by microorganisms in nature, which reduces its environmental impact. Starch is a type of polysaccharide, a carbohydrate produced by plants and some microorganisms that contributes to sustainability [7, 8]. It is a macromolecule composed of a large number of glucose molecules bonded together and is often made up of two major components: amylose and amylopectin. Soni et al. reported that the biodegradability of cellulose oxide was enhanced by starch blends in their evaluation of marine microbial degradation of cellulose oxide films [9]. As a result, the addition of starch is considered to accelerate the biodegradability of PLA [10]. To enhance the

Supplementary information The online version contains supplementary material available at <https://doi.org/10.1038/s41428-024-00918-5>.

✉ Yu-I Hsu
yuihsu@chem.eng.osaka-u.ac.jp

¹ Graduate School of Engineering, Osaka University, 2-1 Yamadaoka, Suita, Japan

thermoplasticity of starch in blends with other plastics, thermoplastic starch (TPS) is often plasticized with glycerol or sorbitol. PLA/TPS blends have potential applications in various industries, including food packaging, agriculture, and biomedicine. In particular, food packaging benefits from the mechanical properties and biodegradability of the blend, making it an ideal choice for single-use containers and films [11]. PLA/TPS blends have potential applications in biodegradable mulch films can help reduce plastic waste in agriculture. In the biomedical field, the biocompatibility and biodegradability of the blend make it a promising temporary medical device, drug delivery system, and tissue engineering scaffold [12]. However, PLA and TPS are immiscible owing to the hydrophobicity of PLA and the hydrophilicity of TPS. Because of the poor interfacial affinity and compatibility between TPS and PLA mixtures, the mechanical properties of PLA/TPS blends are inferior to those of neat PLA, which limits their application [13, 14]. Several studies have been performed to improve the compatibility of PLA and TPS. Gómez-Contretas et al. used epoxidized sesame oil (ESO) as a compatibilizer for PLA/TPS blends and found that the interfacial affinity between PLA and TPS was improved owing to the increased molecular interaction caused by the coupling effect of ESO [15]. Yu et al. prepared PLA blends with thermoplastic acetylated starch (TPAS) [16]. When 40 wt% TPAS was added, the elongation at break increased by a factor of > 4, and ductile fracture occurred. However, in these studies, most of the hydroxyl groups of starch were modified by chemical reactions and lost their hydrophilic properties. This affects the biodegradation rate of PLA as well as the enzymatic degradability of starch, as it is less likely to attract microorganisms. Therefore, it is important to control the compatibility of PLA and starch while maintaining the hydroxyl groups in starch. However, the hydroxyl groups in the starch cause stickiness on the surface of the blend material, and the rapid elution of the starch into water reduces the water resistance of the PLA/TPS blend. These issues can negatively affect the development of applications.

In the present study, the effect of adding oligo(lactic acid)-grafted starch (OLAgSt) as a compatibilizer to PLA/TPS blends to improve the compatibility of PLA and starch and increase water resistance while maintaining many of the hydroxyl groups in starch was evaluated. OLAgSt was expected to not only biodegrade but also improve the compatibility of PLA and TPS without affecting the biodegradability of PLA/TPS. It was synthesized in a one-pot bulk reaction via the ring-opening polymerization of lactide using the hydroxyl group of starch as an initiator. This polymerization can preserve a large number of starch hydroxyl groups because only the surface of starch particles is modified with OLA. Fourier transform infrared

(FT-IR) spectroscopy and proton nuclear magnetic resonance ($^1\text{H-NMR}$) spectroscopy were used to characterize the samples and calculate the degree of substitution (DS) of OLAgSt and the molecular weight of OLA. Additionally, PLA/TPS with OLAgSt blends were prepared via melt kneading and molding of the blend films. For the blended films, the effect of OLAgSt addition and the influence of the DS and OLA molecular weight in OLAgSt were evaluated by scanning electron microscopy (SEM), water contact angle measurements, water resistance measurements, and tensile tests. This is a new technological approach that allows for improvement of physical properties without changing the conventional melt blending process.

Experimental section

Materials

PLA (2003D) was obtained from NatureWorks LLC (Minnesota, USA). The melt flow rate (MFR) was 6 g/10 min (210 °C, 2.16 kg). TPS, i.e., corn starch-plasticized with glycerol, was supplied by Sankyo Chemical Industry Co., Ltd. (Osaka, Japan). Tapioca starch was supplied by Matsutani Chemical Industry Co., Ltd. (Hyogo, Japan). L-lactide and tin(II) 2-ethylhexanoate ($\text{Sn}(\text{Oct})_2$) were obtained from Tokyo Chemical Industry Co., Ltd. (Tokyo, Japan). Aniline, ammonium chloride (NH_4Cl) and sodium phosphate (NaHPO_4) and N-allylthiourea were purchased from FUJIFILM Wako Pure Chemical Co. (Osaka, Japan). All reagents were used as received without further purification.

Polymerization of OLAgSt

OLAgSt was synthesized by ring-opening polymerization of L-lactide using the hydroxy group of tapioca starch as an initiator. Starch and L-lactide were mixed in a three-necked flask under vacuum and dried for 2 h at room temperature. The mixture was subsequently heated to 180 °C under a nitrogen atmosphere and polymerized for 3 h using $\text{Sn}(\text{Oct})_2$ as a catalyst. Then, the mixture was reprecipitated using chloroform and excess methanol to remove the unreacted lactide monomer and catalyst. OLAgSt and the PLA homopolymer were separated via Soxhlet extraction with toluene for 24 h and then filtered. The remaining solids were washed with toluene and dried under vacuum at 80 °C for 4 h. The obtained OLAgSt was characterized via FT-IR and $^1\text{H-NMR}$ spectroscopy. Three types of OLAgSt were synthesized with different lactic acid chain lengths and DSs, and the feed ratios and catalyst amounts are presented in Table 1.

Table 1 Synthesized OLA_gSt

Sample code	Starch [g]	L-Lactide [g]	Catalyst [starch per wt%]
OLA _g St-a	10	30	0.050
OLA _g St-b	10	30	0.225
OLA _g St-c	20	20	0.225

Preparation of the PLA/TPS-OLA_gSt blend film

PLA, TPS, and OLA_gSt were dried under vacuum at 80 °C for 4 h to remove water from the sample before blending. PLA/TPS-OLA_gSt blends were prepared via melt kneading using a twin-screw internal mixer (Labo Plastmill 4C150-01, Toyo Seiki Co., Ltd. Tokyo, Japan) at 170 °C for 10 min with a screw speed of 70 rpm. The obtained blends were transformed into 0.5-mm thick films via hot pressing at 180 °C for 5 min at a pressure of 20 MPa. PLA/TPS-OLA_gSt blend films with different compositions were prepared, as shown in Table 2.

Measurements

FT-IR spectroscopy was performed using a Nicolet iS5 instrument (Thermo Fisher Scientific, Inc., Massachusetts, USA) with attenuated total reflectance. ¹H-NMR (Bruker AVANCE III 600 MHz, Bruker Corporation, Massachusetts, USA) spectra of three types of OLA_gSt were recorded to analyze the chemical changes resulting from the reaction. The samples were dissolved in deuterated dimethyl sulfoxide (DMSO-_{d6}) at 50 °C and sealed in 5-mm NMR analysis tubes with a ratio of 10 mg of solid sample to 1 mL of solvent. The ¹H-NMR spectra were collected from 0 to 7 ppm.

The mechanical properties of the various blends were evaluated via tensile tests at room temperature using an AutoGraph AGS-X (Shimadzu Co., Kyoto, Japan) with a constant deformation rate of 10 mm/min. The samples were cut into dumbbell-shaped sheets (W 4 mm × D 20 mm) with a thickness of approximately 0.5 mm.

The morphologies of the blend film surfaces were investigated via SEM (SU3500, Hitachi High-Tech Corporation., Tokyo, Japan) at an accelerating voltage of 15 kV. The samples were coated via platinum sputtering (MSP-1S, VACUUM DEVICE Co., Ltd., Ibaraki, Japan) before being loaded into the SEM device.

The contact angles between the blend films and water droplets (1.0 μL) at room temperature were measured using a contact angle meter (DM300, Kyowa Interface Science Co. Ltd., Saitama, Japan). Images were captured after 10 s to reach a steady state.

To evaluate the water resistance, the weight loss of the blend film in water was measured. Before the test, the initial

Table 2 Compositions of the PLA/TPS-OLA_gSt blend films

Sample	PLA/TPS [w/w]	OLA _g St	
			[wt%]
PLA/TPS	80/20	–	0
PLA/TPS-2OLA _g St-a		OLA _g St-a	2
PLA/TPS-4OLA _g St-a		OLA _g St-a	4
PLA/TPS-6OLA _g St-a		OLA _g St-a	6
PLA/TPS-2OLA _g St-b		OLA _g St-b	2
PLA/TPS-4OLA _g St-b		OLA _g St-b	4
PLA/TPS-6OLA _g St-b		OLA _g St-b	6
PLA/TPS-2OLA _g St-c		OLA _g St-c	2
PLA/TPS-4OLA _g St-c		OLA _g St-c	4
PLA/TPS-6OLA _g St-c		OLA _g St-c	6

weight (W₁) of each film (20 mm × 20 mm × 0.5 mm) was measured. The films were immersed in water at room temperature. After a few days, the insoluble remains of the films were dried under vacuum at 80 °C for 4 h. Finally, the insoluble dried films were weighed (W₂). The weight loss was calculated using Eq. (1). Measurements were performed for 7 d.

$$\text{Weight loss (\%)} = [1 - (W_1 - W_2)/W_2] \times 100 \quad (1)$$

Biochemical oxygen demand (BOD) testing according to OECD 306 was used to evaluate the marine degradability of PLA/TPS with OLA_gSt blends. Seawater was collected from the sea in Hyogo Prefecture (34°71'N, 135°35'E). Seawater was collected on March 8, 2024, with a water temperature of 15.2 °C. The tests were conducted in a pressure sensor- type BOD reactor (6D, TAITEC Co., Ltd., Saitama, Japan) in the dark at 20 °C for 28 days. Aniline was used as a reference. Each BOD reactor contained 10 mg of aniline or a 10 × 10 × 0.5 mm thick sample film, along with 100 ml of seawater and nutrients (25 mg of NH₄Cl, 5 mg of NaHPO₄, 0.5 mg of N-allylthiourea, and 0.1 mL of a buffer solution) to ensure unrestricted conditions for microbial activity and growth. Equation (2) was used to calculate the BOD biodegradability, where BOD_s represents the BOD of the sample, and BOD_{blank} represents the BOD of a reactor that contains nothing. ThOD refers to the theoretical oxygen demand. The ThOD of PLA, starch, and glycerol were 1.33, 1.19, and 1.22, respectively. The ThOD of OLA_gSt was calculated to be the same as that for starch because the oxygen demand from OLA is negligible due to its low degree of substitution.

$$\text{BOD (\%)} = \frac{\text{BOD}_s - \text{BOD}_{\text{blank}}}{\text{ThOD}} \times 100 \quad (2)$$

Results & discussion

Characterization of OLA_gSt

OLA_gSt was synthesized by ring-opening polymerization at different starch and L-lactide feed ratios. The FT-IR spectra of starch and OLA_gSt are shown in Fig. 1. After ring-opening polymerization with L-lactide, a new peak at 1735 cm⁻¹ (C=O stretching) was observed for OLA_gSt compared with starch. This peak is attributed to the ester linkages of OLA. Additionally, the intensity of the peak attributed to the hydroxyl groups in starch (3400 cm⁻¹) decreased owing to the hydroxyl groups acting as initiators of the ring-opening polymerization of OLA. OLA_gSt-a and OLA_gSt-b were found to have good OLA modification, as their peaks were hardly observed. However, for OLA_gSt-c, the peak from hydroxy groups in starch was still present,

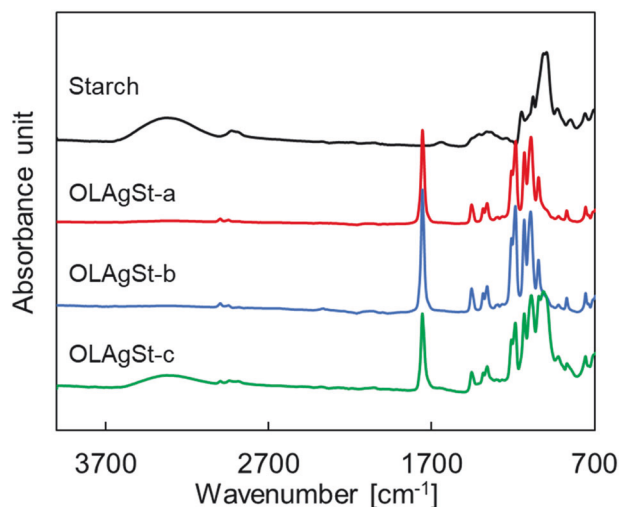


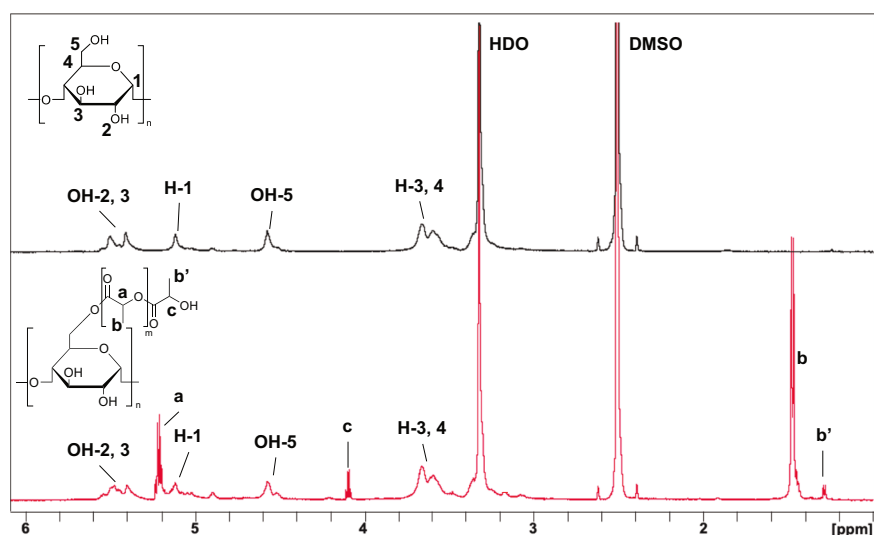
Fig. 1 Infrared spectra of starch and OLA_gSt

likely because of the low DS. Figure 2 shows the ¹H-NMR patterns of starch and OLA_gSt-a, with the peaks of starch-derived pyranose protons exhibiting chemical shifts (δ) of 3.0–4.0 and 5.1 ppm. In contrast, OLA_gSt-a exhibited new peaks at δ = 1.3, 1.5, 4.1, and 5.2 ppm, which are attributed to the internal and terminal methine groups of OLA, as well as the internal methyl groups [17–19]. Table 3 presents the DS and number average molecular weight (M_n) calculated using the ¹H-NMR spectra of OLA_gSt and the yield. The DS was calculated by taking the integral ratio of the OLA-terminal methylene peak (b') to the pyranose proton peak (H-1), while the M_n was calculated by taking the integral ratio of the OLA-terminal methylene peak (b') to the repeated methylene peak (b). OLA_gSt-a exhibited the highest DS, while OLA_gSt-b exhibited the highest M_n, indicating that the amount of catalyst and feed ratio of L-lactide can control the DS and M_n of OLA. OLA_gSt-c exhibited a lower DS and M_n of OLA owing to the smaller amount of L-lactide relative to starch during the ring-opening polymerization. Additionally, the yield was lower for OLA_gSt-c than for OLA_gSt-a and OLA_gSt-b. The OLA_gSt-c feed ratio resulted in the generation of a significant amount of unreacted lactide and homopolymer that did not react with the starch. Furthermore, OLA_gSt-c did not exhibit thermoplasticity because of its low DS and OLA, whereas OLA_gSt-a and OLA_gSt-b exhibited thermoplasticity.

Table 3 Characterization of three types of OLA_gSt

Sample	DS	M _n of OLA	Yield [%]
OLA _g St-a	0.46	1010	43.2
OLA _g St-b	0.27	1800	45.7
OLA _g St-c	0.11	730	47.2

Fig. 2 ¹H-NMR spectra of starch and OLA_gSt-a



Mechanical properties of PLA/TPS with the OLA_gSt blend

Tensile tests were performed to evaluate the impact of the addition of OLA_gSt to PLA/TPS blends on the mechanical properties. Table 4 presents the mechanical properties of the PLA/TPS-OLA_gSt blends evaluated via tensile tests. The Young's modulus and maximum stress increased with the amount of OLA_gSt added to PLA/TPS. The increase in Young's modulus was proportional to the amount of OLA_gSt added. The addition of OLA_gSt improved the interfacial adhesion between TPS and PLA, enhancing the filler effect of TPS [20]. However, the elongation at break decreased as the OLA_gSt content increased, and the maximum stress occurred at 4 wt% OLA_gSt. This is because the addition of OLA_gSt increased the total starch content of the blend sample. Because starch is a rigid filler, the increase in starch led to stress concentration and promoted breakage. This result indicated that excess OLA_gSt degrades the mechanical properties. The lowest elongation at break was observed for PLA/TPS-6OLA_gSt-c. It was suggested that OLA_gSt-c was not homogeneously dispersed within PLA because it does not exhibit thermoplasticity. OLA_gSt-c did not function as a compatibilizer between PLA and TPS as intended. The large variability in the maximum stress and Young's modulus indicated the heterogeneous dispersion of OLA_gSt-c. No differences in mechanical properties were observed between OLA_gSt-a and OLA_gSt-b.

Morphology of PLA/TPS with the OLA_gSt blend

To evaluate the compatibility and the inhibition of surface exposure of starch in the PLA/TPS blend with the addition of OLA_gSt, the morphologies of the film surface and tensile fracture surface were observed. The prepared films were examined by capturing photographs and SEM images, as shown in Figs. 3 and 4, respectively. In Fig. 3, the films are homogeneous, except for PLA/TPS-6OLA_gSt-c, which has

a slight brown color because of OLA_gSt-c. It is considered to be thermally degraded owing to the prolonged exposure of starch with many hydroxyl groups to high temperatures during the synthesis of OLA_gSt. Additionally, the lack of thermoplasticity in OLA_gSt-c resulted in agglomeration within the film.

Native starch does not have plasticity owing to its intra- and intermolecular hydrogen bonds, resulting in granule sizes of 10–40 μm [21]. In comparison, PLA/TPS exhibited larger dispersed granules (approximately 50 μm), as shown in Fig. 4. This is attributed to the significant difference in melt viscosity between PLA and TPS, as well as the high interfacial resistance. The melt viscosity of TPS was too high to measure the MFR under the same conditions used for PLA. Wu's empirical equation (Eq. (3)) supports this hypothesis [22].

$$R = 4(\sigma/\gamma \cdot \eta_m)(\eta_d/\eta_m)^{\pm 0.84} \quad (3)$$

Here, R represents the dispersed particle size, σ represents the interfacial tension, γ represents the shear rate, η_m represents the melt viscosity of the continuous-phase component, and η_d represents the melt viscosity of the dispersed-phase component. According to Eq. (3), the size of dispersed particles increases when the interfacial tension or the ratio of the melt viscosity of the continuous phase to that of the dispersed phase is high [23]. In the film sample containing OLA_gSt-a and OLA_gSt-b, as the OLA_gSt

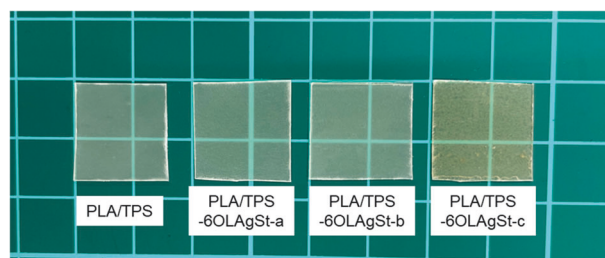
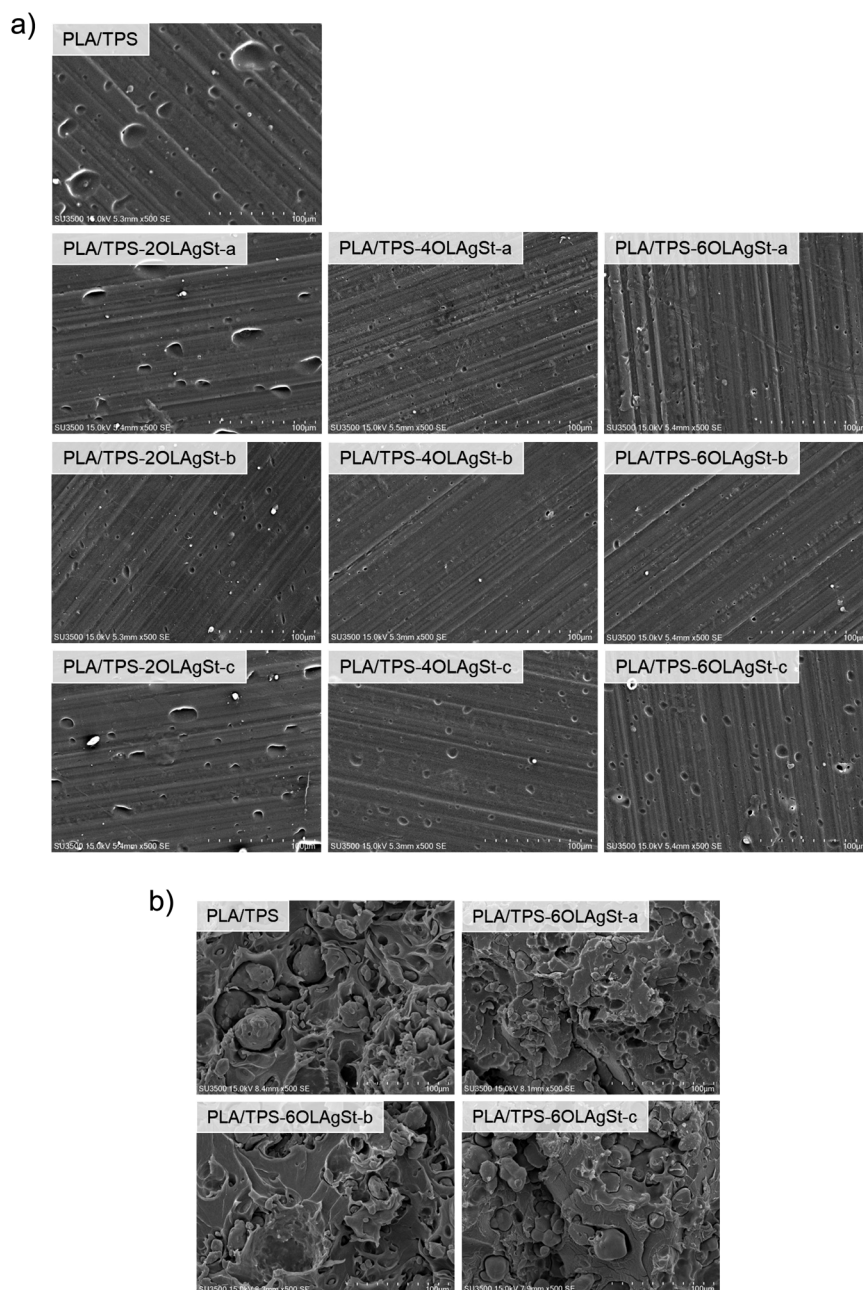


Fig. 3 Prepared films consisting of PLA/TPS and 6 wt% OLA_gSt

Table 4 Mechanical properties of the PLA/TPS-OLA_gSt films evaluated via tensile tests

Sample	Young's modulus [MPa]	Maximum stress [MPa]	Strain at break [%]
PLA/TPS	2120.2 ± 119.1	36.2 ± 3.0	2.52 ± 0.47
PLA/TPS-2OLA _g St-a	2192.7 ± 46.3	36.1 ± 2.4	2.22 ± 0.38
PLA/TPS-4OLA _g St-a	2259.4 ± 37.5	38.4 ± 0.5	2.15 ± 0.05
PLA/TPS-6OLA _g St-a	2280.2 ± 71.9	36.0 ± 2.2	2.17 ± 0.31
PLA/TPS-2OLA _g St-b	2214.0 ± 46.1	34.8 ± 2.5	2.53 ± 0.53
PLA/TPS-4OLA _g St-b	2268.8 ± 48.9	40.7 ± 2.3	2.18 ± 0.10
PLA/TPS-6OLA _g St-b	2245.9 ± 48.8	38.4 ± 0.7	2.17 ± 0.08
PLA/TPS-2OLA _g St-c	2261.6 ± 58.4	37.3 ± 1.8	2.36 ± 0.39
PLA/TPS-4OLA _g St-c	2257.4 ± 51.6	36.3 ± 3.0	2.20 ± 0.51
PLA/TPS-6OLA _g St-c	2340.0 ± 89.9	33.6 ± 8.9	1.80 ± 0.46

Fig. 4 SEM images of **a** the film surface and **b** the tensile fracture surface of the PLA/TPS-OLAgSt films



content increased, the TPS granule size decreased, and the dispersion within PLA improved. Specifically, the TPS granule size observed at the tensile fracture surface was 18 μm for PLA/TPS-6OLAgSt-a and 25 μm for PLA/TPS-6OLAgSt-b. Additionally, the area of TPS exposed on the film surface decreased. The reduction in granule size and improved dispersibility enhanced the stability of the blend, even as the TPS and PLA interface increased. Therefore, OLASt-a and OLASt-b functioned as compatibilizers for PLA and TPS. The microdispersion of hydrophilic TPS

within hydrophobic PLA indicated that OLASt-a and OLASt-b acted on the surface of TPS. This behavior was also observed on the fracture surface inside the film. The dispersibility of TPS on the film surface was better for PLA/TPS-2OLAgSt-b than for PLA/TPS-2OLAgSt-a. OLASt-b had a greater improvement in compatibility than OLASt-a. OLASt-c slightly improved the dispersion of TPS but increased the area of TPS exposed on the film surface. OLASt-c did not function well as a compatibilizer owing to its lack of thermoplasticity and low OLA content.

Water contact angle of the film surface

The water contact angle was used to confirm the hydrophobicity or hydrophilicity of the blend film. Figure 5 shows the water contact angles of the PLA/TPS blends with OLA_gSt. The contact angle of PLA (106.9°) indicated hydrophobicity. However, blending with TPS resulted in hydrophilicity (81.5°) owing to the large area of hydroxy groups of TPS exposed on the film surface. This hydrophilicity was considered to cause stickiness on the PLA/TPS film surface. Moreover, the addition of OLA_gSt-a and OLA_gSt-b to PLA/TPS resulted in contact angles > 90°, significantly improving the surface properties of the polymer blend. Thus, the addition of only 2 wt% OLA_gSt-a and OLA_gSt-b is effective for improving the stickiness of the film. Furthermore, increasing the content of OLA_gSt-a and OLA_gSt-b resulted in contact angles almost identical to those of PLA. The results indicated that OLA_gSt-a and OLA_gSt-b protect the hydroxyl group of TPS by covering the surface of the TPS granules. However, in films with the addition of OLA_gSt-c, increasing the OLA_gSt-c content reduced the contact angle. PLA/TPS-6OLA_gSt-c exhibited a smaller contact angle than did PLA/TPS, indicating a more hydrophilic film surface. Importantly, the contact angle is affected by not only the solvent affinity but also the

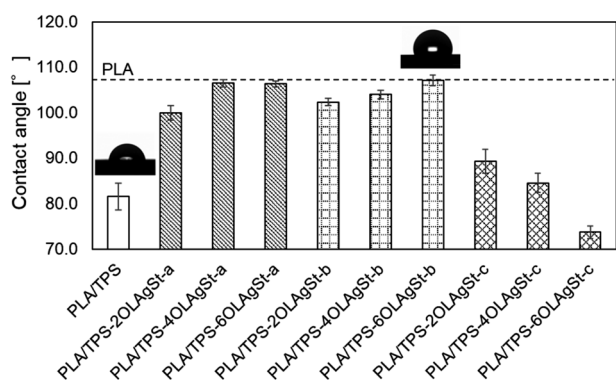


Fig. 5 Water contact angles of the PLA/TPS-OLA_gSt films

surface roughness of the film. A more uniform hydrophilic surface results in a smaller water contact angle. Therefore, an increase in the OLA_gSt-c content led to an increase in the film surface roughness. The SEM observations supported the finding that OLA_gSt-c is not a compatibilizer but shares characteristics with starch because of its extremely low DS.

Water resistance and marine biodegradability of PLA/TPS with the OLA_gSt blend

An immersion test of the blended films was conducted to evaluate their short-term water resistance. Figure 6 shows the weight loss after immersion for up to 7 d. All the samples lost approximately 6 wt% after 1 d of immersion, which agreed well with the amount of glycerol added as a plasticizer in the TPS. Therefore, it was considered that glycerol, which is hydrophilic, leaked into the water in a short period. The results indicate that there is no strong interaction between OLA_gSt and glycerol. Esmaeili et al. reported that in PLA/TPS blends, glycerol as a plasticizer permeates into PLA, suggesting that there is no strong interaction between OLA_gSt and glycerol [24]. It was considered that OLA_gSt localizes on the starch surface and thus cannot prevent the elution of glycerol in PLA. However, the effect of OLA_gSt addition was observed after 3 d of immersion. The addition of OLA_gSt-a and OLA_gSt-b prevented up to 77% of the weight loss compared with no addition of OLA_gSt. This weight loss is attributed to the elution of starch. OLA_gSt improved the starch dispersion and reduced the elution despite increasing the specific surface area of the starch. This is attributed to OLA_gSt covering the starch and the starch surface being hydrophobic, as well as the improved interfacial affinity with PLA. The results of the contact angle measurements were consistent with those obtained with the addition of OLA_gSt, indicating modification of the film surface and an increase in the long-term water resistance. Compared with OLA_gSt-a, OLA_gSt-b exhibited better improvements in morphology and water

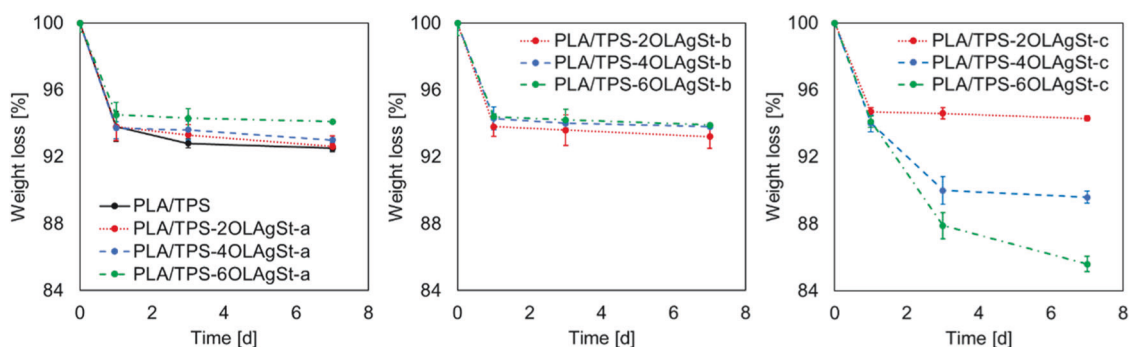


Fig. 6 Weight loss of the PLA/TPS-OLA_gSt films

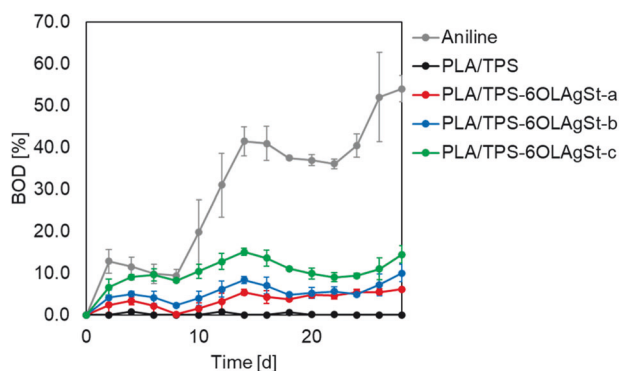


Fig. 7 The marine biodegradability of PLA/TPS-OLAgSt films

contact angle at a smaller addition amount. The effect of OLAgSt as a compatibilizer depends more strongly on the molecular weight of OLA than the DS. On the other hand, OLAgSt-c accelerated the weight loss of PLA/TPS. This was attributed to the increase in TPS granules and OLAgSt-c on the film surface, which are easily leached out due to low interfacial adhesion with PLA.

As a representative sample, the biodegradability of PLA/TPS and 6 wt% OLAgSt-added blends were evaluated in a seawater environment (Fig. 7). During 28-day period, only 54% of the aniline, which was used as a standard sample, was biodegraded. It was suggested that there were few active microorganisms in the cold seawater sample collected. The biodegradability of PLA/TPS was limited, but it was improved by the addition of OLAgSt. The BOD values of the OLAgSt-a and OLAgSt-b blends were 6.2% and 10.0%, respectively. This improvement was attributed to the increased surface area of the TPS granules resulting from the addition of OLAgSt and the resulting increase in the contact area with seawater. OLAgSt-c did not act as a compatibilizer for PLA or TPS, but it significantly improved the biodegradability of PLA/TPS (BOD = 14.5%). This improvement is attributed to the increased amount of starch on the film surface resulting from the addition of OLAgSt-c, which made the film hydrophilic and created an environment suitable for microbial attraction. For PLA/TPS-6OLAgSt-c, the theoretical BOD attributed to TPS and OLAgSt was 12.6%. Therefore, both TPS and a small amount of PLA might have been biodegraded. This is a new finding that contradicts the previously reported finding that PLA is not biodegradable in freshwater or seawater. Palai et al. reported that the biodegradability of PLA/TPS in soil is due to the aggregation of microorganisms on the blended film to degrade TPS, creating a rich microbial environment. It has been suggested that this abundance of microorganisms degrades PLA [10]. The biodegradability of PLA/TPS films is greater for OLAgSt-c than for PLA alone. This was attributed to the hydrophilic nature of the PLA/TPS film, which promoted microbial

aggregation. These results indicate that the marine biodegradability of PLA/TPS is strongly influenced by the dispersibility of TPS and the hydrophilicity of the blend surface.

Conclusion

OLAgSt was prepared by ring-opening polymerization of L-lactide using the hydroxy group of starch as an initiator. Adding 4 wt% OLAgSt significantly improved the compatibility of TPS and PLA, as well as the water resistance and Young's modulus of the PLA/TPS blend. The compatibilizing effect of OLAgSt on PLA/TPS blends depended on the molecular weight of OLA and the DS of the starch. The compatibility of TPS and PLA improved to a greater extent with increasing OLA molecular weight. OLAgSt covered the TPS surface, which improved its water resistance. However, this additive was not effective against glycerol, which is a plasticizer of TPS. OLAgSt-added PLA/TPS blends are promising for applications in food packaging, e.g., biodegradable gas barrier films.

Supporting information is available at (Improvement in the physical properties of poly(lactic acid)/thermoplastic starch blends using oligo(lactic acid)-grafted starch)'s website' at the end of the article and before the references.

Acknowledgements This work was supported by Japan Science and Technology Agency Grants (JPMJPF2218), the Environment Research and Technology Development Fund JPMEERF21S11900 of the Environmental Restoration and Conservation Agency of Japan, and JSPS KAKENHI Grants (23H02024), JST PRESTO (JPMJPR23N4), and JST SPRING (JPMJSP2138).

Author contributions K.S.: Investigation, Writing - original draft, Writing - review & editing, Funding acquisition; Y.H.: Supervision, Writing -review & editing, Funding acquisition; H.U.: Supervision, Writing - review & editing, Funding acquisition

Compliance with ethical standards

Conflict of interest The authors declare no competing interests.

References

1. Jambeck JR, Geyer R, Wilcox C, Siegler TR, Perryman M, Andrady A, et al. Plastic waste inputs from land into the ocean. *Science*. 2015;347:768–71.
2. Devi SS, Sreedevi AV, Kumar AB. First report of microplastic ingestion by the alien fish Pirapitinga (*Piaractus brachipomus*) in the Ramsar site Vembanad Lake, south India. *Mar Pollut Bull*. 2020;160:111637.
3. Jian J, Xiangbin Z, Xianbo H. An overview on synthesis, properties and applications of poly(butylene-adipate-co-terephthalate)-PBAT. *Adv Ind Eng Polym Res*. 2020;3:19–26.
4. Garlotta D. A literature review of poly(Lactic Acid). *J Polym Environ*. 2001;9:2.

5. Muller J, González-Martínez C, Chiralt A. Combination of poly(lactic) acid and starch for biodegradable food packaging. *Materials*. 2017;10:952.
6. Cristina RC, Rebeca MF, Marola SY, Xosé Antón ÁS. Leaching and bioavailability of dissolved organic matter from petrol-based and biodegradable plastics. *Mar Environ Res*. 2022;176:105607.
7. Zhu F. Structures, properties, modifications, and uses of oat starch. *Food Chem*. 2017;229:329–40.
8. Shazia T, Younas M, Zaeem MA, Majeed I, Noreen A, Iqbal MN, et al. A review on blending of corn starch with natural and synthetic polymers, and inorganic nanoparticles with mathematical modeling. *Int J Biol Macromol*. 2019;122:969–96.
9. Soni R, Asoh TA, Hsu YI, Uyama H. Freshwater-durable and marine-degradable cellulose nanofiber reinforced starch film. *Cellulose*. 2022;29:1667–78.
10. Palai B, Mohanty S, Nayak SK. A comparison on biodegradation behaviour of polylactic acid (PLA) based blown films by incorporating thermoplasticized starch (TPS) and Poly (Butylene Succinate-co-Adipate) (PBSA) biopolymer in soil. *J Polym Environ*. 2021;29:2772–88.
11. Mangaraj S, Yadav A, Bal LM, Dash SK, Mahanti NK. Application of biodegradable polymers in food packaging industry: a comprehensive review. *J Packag Technol Res*. 2019;3:77–96.
12. Saini P, Arora M, Kumar MNVR. Poly(lactic acid) blends in biomedical applications. *Adv Drug Deliv Rev*. 2016;107:47–59.
13. Wang N, Yu J, Chang PR, Ma X. Influence of formamide and water on the properties of thermoplastic starch/poly(lactic acid) blends. *Carbohydr Polym*. 2008;71:109–18.
14. Ferrarezi MMF, De Oliveira Taipina M, Escobar Da Silva LC, Gonçalves MDC. Poly(ethylene glycol) as a compatibilizer for poly(lactic acid)/thermoplastic starch blends. *J Polym Environ*. 2013;21:151–9.
15. Gómez-Contreras P, Contreras-Camacho M, Avalos-Belmontes F, Collazo-Bigliardi S, Ortega-Toro R. Physicochemical properties of composite materials based on thermoplastic yam starch and polylactic acid improved with the addition of epoxidized sesame oil. *J Polym Environ*. 2021;29:3324–34.
16. Yu M, Zheng Y, Tian J. Study on the biodegradability of modified starch/polylactic acid (PLA) composite materials. *RSC Adv*. 2020;10:26298–307.
17. Shao A, Zhao J, Zhao Y, Yan Y, Qiu Z. A facile way to synthesize polylactide grafted starch: anionic swollen polymerization. *Polym Bull*. 2013;70:59–70.
18. Wang Q, Hu Y, Zhu J, Liu Y, Yang X, Bian J. Convenient synthetic method of starch/lactic acid graft copolymer catalyzed with sodium hydroxide. *Bull Mater Sci*. 2012;35:415–8.
19. Gong Q, Wang LQ, Tu K. In situ polymerization of starch with lactic acid in aqueous solution and the microstructure characterization. *Carbohydr Polym*. 2006;64:501–9.
20. Wootthikanokkhan J, Kasemwananimit P, Sombatsomporn N, Kositchaiyong A, Ayutthaya SI, Kaabuuathong N. Preparation of modified starch-grafted poly(lactic acid) and a study on compatibilizing efficacy of the copolymers in poly(lactic acid)/thermoplastic starch blends. *J Appl Polym Sci*. 2012;126:389–96.
21. Corgneau M, Gaiani C, Petit J, Nikolova Y, Banon S, Ritte-Pertusa L, et al. Digestibility of common native starches with reference to starch granule size, shape and surface features towards guidelines for starch-containing food products. *Int J Food Sci Technol*. 2019;54:2132–40.
22. Wu S. Formation of dispersed phase in incompatible polymer blends: Interfacial and rheological effects. *Polym Eng Sci*. 1987;27:335–43.
23. Li J, Luo X, Lin X, Zhou Y. Comparative study on the blends of PBS/thermoplastic starch prepared from waxy and normal corn starches. *Starch*. 2013;65:831–9.
24. Esmaeili M, Pircheraghi G, Bagheri R, Altstädt V. Poly(lactic acid)/coplasticized thermoplastic starch blend: Effect of plasticizer migration on rheological and mechanical properties. *Polym Adv Technol*. 2019;30:839–51.

Publisher's note Springer Nature remains neutral with regard to jurisdictional claims in published maps and institutional affiliations.

Springer Nature or its licensor (e.g. a society or other partner) holds exclusive rights to this article under a publishing agreement with the author(s) or other rightsholder(s); author self-archiving of the accepted manuscript version of this article is solely governed by the terms of such publishing agreement and applicable law.